Journal of Non-Crystalline Solids 527 (2020) 119708

Contents lists available at ScienceDirect

Journal of Non-Crystalline Solids

journal homepage: www.elsevier.com/locate/jnoncrysol

Effect of Li_2O–Al_2O_3–GeO_2–P_2O_5 glass crystallization on stability versus molten lithium

S.V. Pershina[a,*], E.A. Il'ina[a], K.V. Druzhinin[a,b], A.S. Farlenkov[a,b]

[a] Institute of High Temperature Electrochemistry of the Ural Branch of the RAS, 20 Akademicheskaya street, Ekaterinburg 620990, Russia
[b] Ural Federal University named after the First President of Russia B. N. Yeltsin, 19 Mira street, Ekaterinburg 620002, Russia

ARTICLE INFO

Keywords:
All-solid-state lithium batteries
Glass
Glass-ceramics
Ionic conductivity
NASICON-type structure

ABSTRACT

Glass and glass-ceramic NASICON-type electrolytes of $Li_{1.5}Al_{0.5}Ge_{1.5}(PO_4)_3$ composition were obtained by melt quenching and glass crystallization, respectively. The stability of the solid electrolytes to molten metallic Li was studied by immersing the samples and holding them at 230 °C for 72 h. Li|glass|Li and Li|glass-ceramics|Li electrochemical cells were assembled and their resistance was measured by impedance spectroscopy at 200 °C for 9 days. It was established that, unlike the glass, the glass-ceramics did not change in its phase composition and molecular structure after the tests. It is shown that $Li_{1.5}Al_{0.5}Ge_{1.5}(PO_4)_3$ glass-ceramics is chemically stable in contact with metallic Li.

1. Introduction

Nowadays lithium-ion and lithium batteries are the most popular power sources both for portable electronics and in large-scale applications [1]. Commercially produced lithium-ion batteries use liquid or gel polymer electrolytes which have a number of disadvantages: flammability, thermal instability and a potential dendrite formation [1–3]. In this regard, solid electrolytes that have a high Li-ion conductivity (not lower than 10^{-4} S/cm at temperatures close to ambient), low porosity and stability in contact with electrode materials look very promising.

High-conductivity Li^+ solid electrolytes are found among NASICON-structured conductors with the general formula $LiM_2(PO_4)_3$, where M = Ti, Ge, Zr, Hf or Sn [1,4]. For example, one compound of this class $Li_{1.3}Al_{0.3}Ti_{1.7}(PO_4)_3$ has a total conductivity of $7{\cdot}10^{-4}$ S/cm at room temperature, but conductors based on lithium titanium phosphate are not stable in contact with Li anode [4]. On the other hand, Al-doped lithium germanium phosphates, in particular, the system $Li_{1+x}Al_xGe_{2-x}(PO_4)_3$, are stable versus metallic Li and have a high Li-ion conductivity [5,6]. When Ge^{4+} is partially replaced by Al^{3+}, the conductivity increases by 3–4 orders of magnitude at room temperature, in which case the region of existence of solid solutions is $0.1 \le x \le 0.6$ [5]. $Li_{1.5}Al_{0.5}Ge_{1.5}(PO_4)_3$ composition (LAGP for short) is reported to have the highest conductivity [7]. However, during a ceramic electrolyte synthesis one cannot avoid the problem of Li penetration into the electrolyte through interconnected pores and grain boundaries accompanied by dendrite growth, and, as a result, a short circuit, which was demonstrated for ceramics based on $Li_7La_3Zr_2O_{12}$ [8]. The mechanism of this phenomenon has not as yet been fully determined, but one of the key factors here may be the nature of lithium diffusion along the grain boundaries of the ceramics and Li precipitation in the intergranular region [9]. A technologically simple way of overcoming this drawback is synthesizing glass-ceramic electrolytes by crystallization of monolithic glass. An advantage of conductors based on phosphate systems is the possibility of the formation of an amorphous phase, from which one can derive a high-conductivity NASICON-structured glass-ceramics, in particular, LAGP. Besides, glass-ceramics has not only a dense microstructure, but also a higher mechanical strength and a lower grain-boundary resistance in comparison with ceramics of analogous composition. However, literature data about the stability of the high-conductivity LAGP electrolyte in contact with metallic lithium are contradictory [6,10], and there are no data regarding the stability of the parent glass.

The present paper reports the synthesis of glass and high-density glass-ceramics $Li_{1.5}Al_{0.5}Ge_{1.5}(PO_4)_3$ with a high Li-ion conductivity and the study of chemical and kinetic compatibility of the obtained solid electrolytes with molten metallic lithium for high-energy Li batteries.

2. Experimental

Glass of $19.75Li_2O$–$6.17Al_2O_3$–$37.04GeO_2$–$37.04P_2O_5$ composition (LAGP for short) was synthesized by melt quenching. Li_2CO_3 (>99.4%), Al_2O_3 (>99.9%), GeO_2 (>99.9%) and $NH_4H_2PO_4$ (≥98.0%) are used

* Corresponding author.
E-mail address: svpershina_86@mail.ru (S.V. Pershina).

https://doi.org/10.1016/j.jnoncrysol.2019.119708
Received 18 March 2019; Received in revised form 11 September 2019; Accepted 23 September 2019
Available online 01 November 2019

as the starting materials. The components were thoroughly mixed together and heated stepwise up to 500 °C to remove volatile substances. Then the resulting mixture was melted in a Pt crucible at 1450 °C for 1 h. The melt was quenched between preheated steel plates. The procedure yielded transparent colorless parallel-sided plates without any impurities. The samples were annealed at 500 °C during 0.5 h to relieve thermal stresses.

$Li_{1.5}Al_{0.5}Ge_{1.5}(PO_4)_3$ glass-ceramics was obtained by glass crystallization. For this purpose, the glass samples were ground on both sides and then crystallized at 820 °C for 8 h in a muffle furnace at the rate of 3 °C/min. After crystallization, the samples were slowly cooled down to room temperature in the furnace. As a result, glass-ceramic samples become white.

The amorphous structure of the original glass and the phase composition of the obtained glass-ceramics were determined by X-ray diffraction method (XRD) with a Rigaku D/MAX-2200VL/PC diffractometer (Rigaku, Japan) over a 2θ range of 10–60° at room temperature. The collected data were processed with the FULLPROF program using ICDD PDF-2 database.

The microstructure of glass-ceramics and glass samples before and after electrochemical experiments were studied by scanning electron microscopy (SEM) using a TESCAN MIRA 3 LMU (TESCAN, Czech Republic). The local microstructure was determined by means of energy dispersive X-ray microanalysis.

The stability of the starting glass and the LAGP glass-ceramics in contact with metallic lithium was determined using two methods: 1) by holding the samples in molten Li with no current applied; 2) electrochemically using Li|solid electrolyte|Li cells at 200 °C for 9 days in the atmosphere of Ar (extra pure grade).

To study the stability of the obtained solid electrolytes, the samples were immersed in molten metallic Li and kept at 230 °C for 72 h. Then the samples were taken from the melt and purified from lithium. Degradation of the samples surface and volume was studied using the XRD and SEM methods. The change in molecular structure was also investigated by Raman spectroscopy using a Raman spectrometer U 1000 (Renishaw, England). The Raman spectra were collected by an Ar-ion laser with a wavelength of 532 nm and a power of 40 mW at a scanning angle of 90°. The Raman spectra were recorded in the static and extended modes in the range of $1200-50\ cm^{-1}$ with spectral resolution of $1\ cm^{-1}$.

To evaluate the degradation of the electrolyte functional properties before and after holding it in molten Li resistance measurements were conducted by impedance spectroscopy in a two-probe cell with silver metal electrodes over the frequency range of 0.025–1000 kHz in air using potentiostats/galvanostat P-5X (Ellins, Russia). Not only the values of resistance at certain temperatures were compared, but also the general appearance of temperature dependences of Li-ion conductivity of the solid electrolytes over a 19–140 °C temperature range. For this purpose, the samples were previously cleaned from residual Li and an Ag-based alloy was sputtered on both ends of the samples to form electrodes.

Li|glass LAGP|Li and Li|glass ceramics LAGP|Li symmetric cells were assembled in a dry argon box M-BROWN (H_2O concentration < 1 ppm). Metallic Li was rolled to the foil with thickness ~150 μm. Electrodes were cut out from the Li foil in the circle form (diameter ~4 mm) in order to avoid the lithium occurrence along the end face of the solid electrolyte sample. The obtained electrodes were pressed by rolling to both polished surfaces of the sample.

The electrical resistance of the studied cells was measured by the complex impedance method using a P-5X galvanostat equipped with FRA24 impedance module (Elins, Russia) in Ar atmosphere at 200 °C for 9 days. Before the each resistance measurement, the lithium | electrolyte interface was electrochemically updated on both sides by a potential difference sweep with speed 10 mV/s for 5–10 cycles (provided a mandatory current response). To establish the presence of electrolyte interaction products with the anode material, the cells were disassembled after electrochemical experiments and evaluated by XRD, Raman spectroscopy and visually by the changing color of the electrolyte.

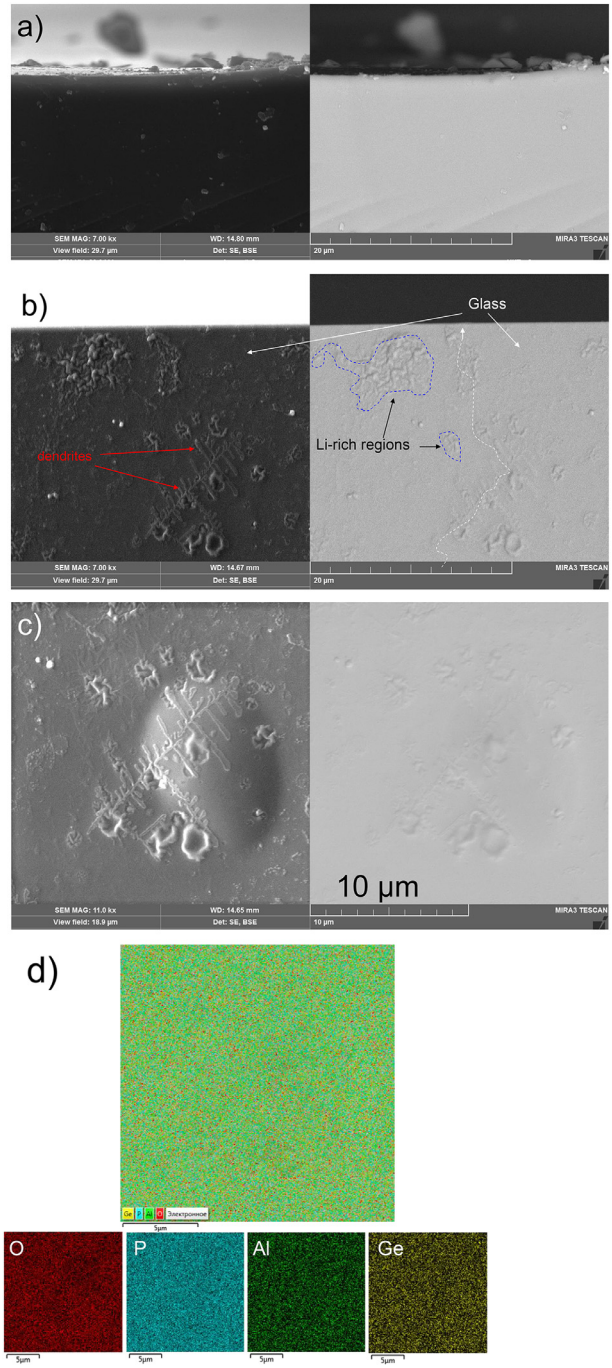

Fig. 1. Cross-section images of the glass before (*a*) and after electrochemical measurements at two different magnification (*b, c*), and the EDS maps of the elements distribution of region *c* (*d*).

3. Results and discussion

3.1. Investigation of the LAGP glass versus molten Li

The first task was to estimate the glass stability versus molten lithium. Glass samples were exposed in contact with lithium pellets at 200 °C for 9 days in cells providing no lithium leakage under melting. SEM picture of the initial glass is shown in Fig. 1a. It can be seen that

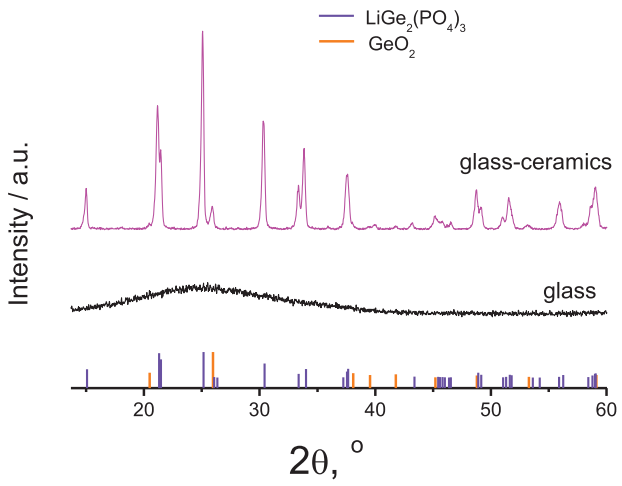

Fig. 2. X-ray diffraction (XRD) patterns of the as-cast glass and the glass-ceramics of $Li_{1.5}Al_{0.5}Ge_{1.5}(PO_4)_3$ composition.

the glass microstructure is homogeneous without interspersed crystalline phases. After exposure pellets in contact with lithium at 200 °C for 9 days, the glass volume was penetrated by dendrites of newly formed phase, as shown in Fig. 1b and c. As initial glass has no significant amount of pores, newly formed phase can not be lithium leaked through glass volume. The results of impedance spectroscopy for the samples also show no short circuit (see Section 3.3). The only way of dendrites nature is the products of chemical reaction between lithium and glass at 200 °C. According to the maps of the element distribution of aluminum, germanium, phosphorus, and oxygen (Fig. 1d), the composition of the newly formed phase does not differ significantly from the glass composition. This may be due to the fact that this phase is enriched in lithium, which can not be evaluated by energy dispersive X-ray microanalysis.

It can be assumed that the parent glass and the product phase have different densities, which leads to the formation of gaps in the glass volume. However, these gaps are wide enough to allow lithium leaking. As lithium fills the gap the new interface between Li and glass forms allowing the reaction expand deeper in the glass volume. Finally the glass penetrates with product phase and the reaction stops when there is not enough lithium. The sample holds its integrity in the cell but it splits up at cell disassembling in the contact area with lithium. To confirm the glass instability several samples were exposed in Li melt at 230 °C for 72 h. It was found that the samples completely dissolved in

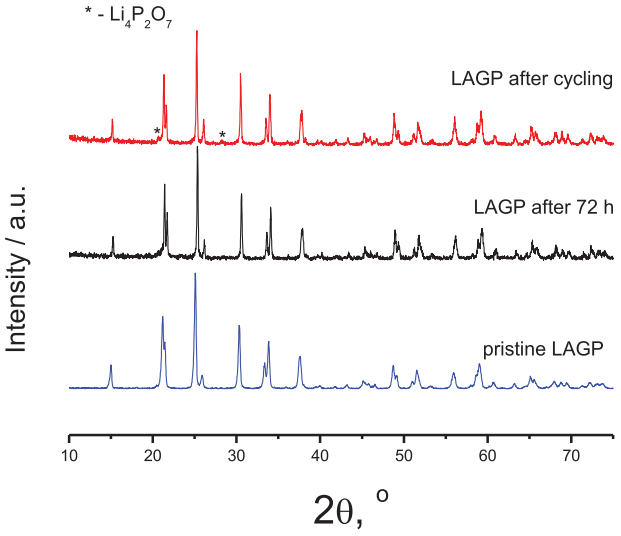

Fig. 4. X-ray diffraction patterns of LAGP glass-ceramics before and after a contact with metallic Li. The asterisk (*) indicates the impurity phase $Li_4P_2O_7$.

molten Li after experiment, no precipitate was either found. Obviously the products of glass reaction with lithium can be dissolved in Li melt.

3.2. Investigation of the LAGP glass-ceramics stability versus molten Li

The obtained glass-ceramics has a NASICON-type structure (Fig. 2) and possesses a high Li-ion conductivity, which was determined by impedance spectroscopy, and is characterized by a dense microstructure. Fig. 2 shows the XRD patterns for the as-cast glass and glass-ceramics of compound $Li_{1.5}Al_{0.5}Ge_{1.5}(PO_4)_3$. The XRD pattern of the glass looks like a halo without any diffraction peaks, which confirms its amorphous nature. The XRD pattern of the LAGP glass-ceramics have peaks corresponding to the conducting phase $LiGe_2(PO_4)_3$ with space group R-3c and the impurity phase GeO_2, Fig. 2. It is known that a partial substitution of Ge^{4+} ions (r_i = 0,53 Å) for Al^{3+} ions (r_i = 0,535 Å) with almost similar ionic radii yields solid solutions $Li_{1+x}Al_xGe_{2-x}(PO_4)_3$ in the interval of $0.1 \leq x \leq 0.6$ [11–13]. As previously reported [14], the GeO_2 impurity phase was always contained in the LAGP glass-ceramics at the crystallization above 578 °C. However, a low content of this impurity does not have a significant effect on the electrical conductivity of the solid electrolyte, which is $(3.9 \pm 0.1)\cdot10^{-4}$ S/cm at 25 °C.

Fig. 3 shows the SEM micrograph of LAGP glass-ceramics. Glass-

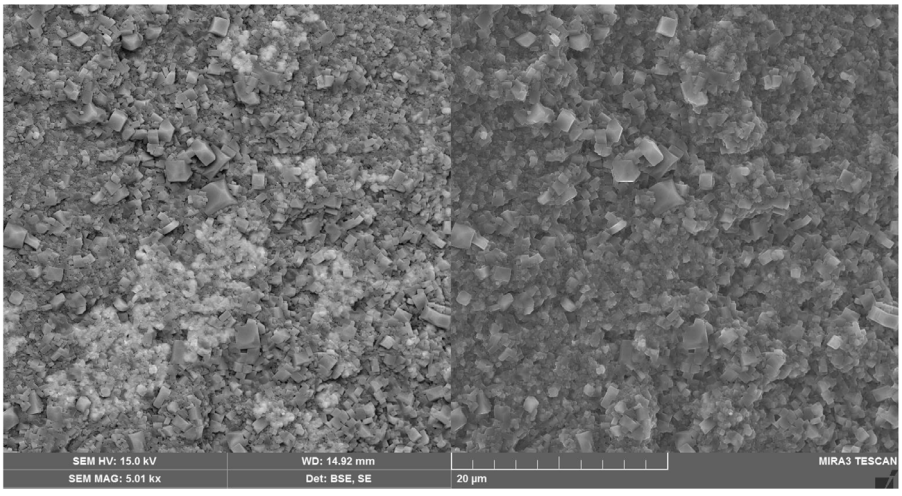

Fig. 3. SEM micrograph of LAGP glass-ceramic sample.

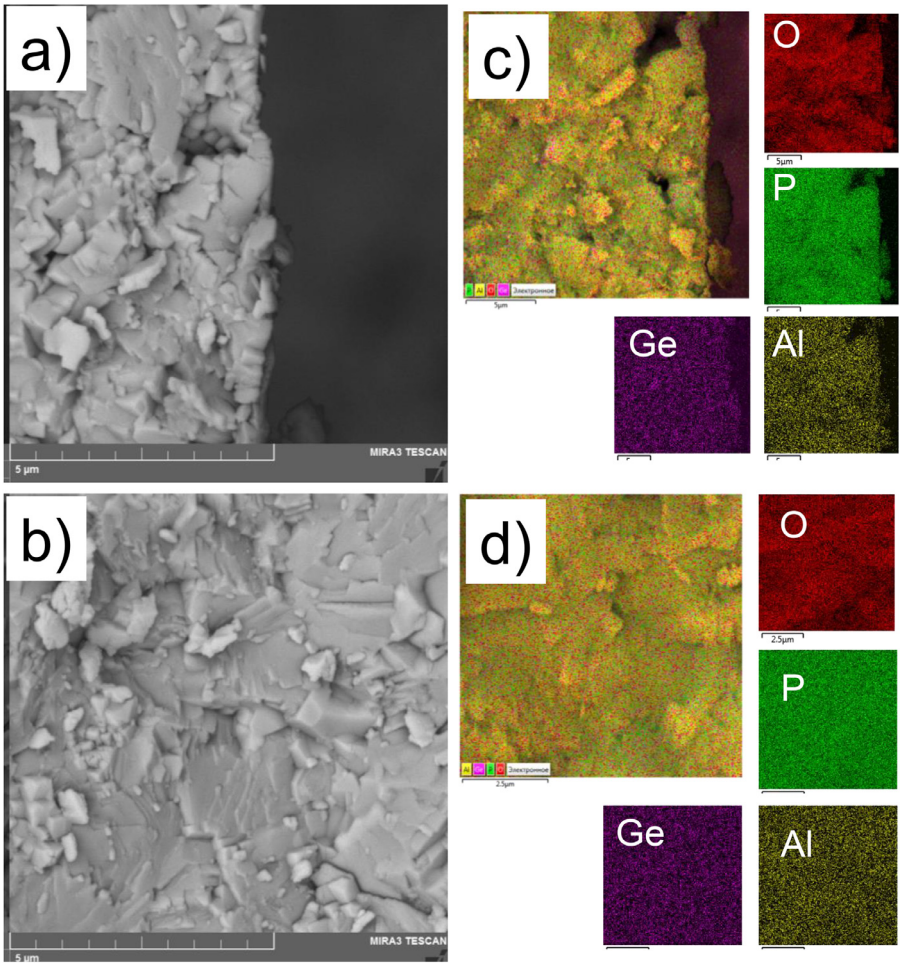

Fig. 5. Cross-section images of the LAGP glass-ceramics obtained after cell testing with metallic Li of *a*) the interface between the Li-metal anode and the glass-ceramics electrolyte, *b*) the volume of sample, and *c, d*) the EDS maps of the elements distribution.

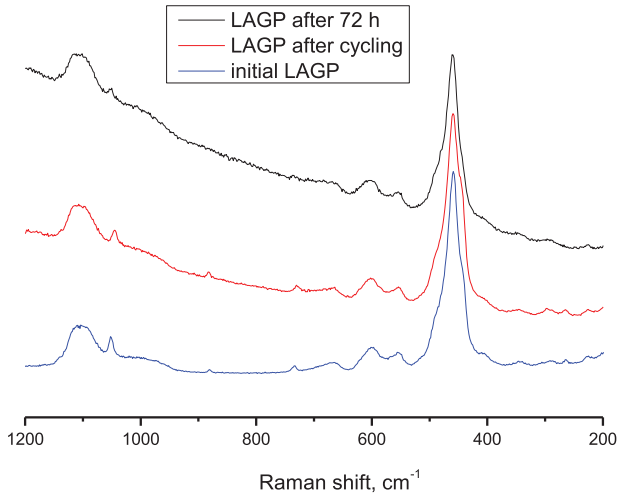

Fig. 6. Raman spectra of the glass-ceramics LAGP before and after testing with metallic Li.

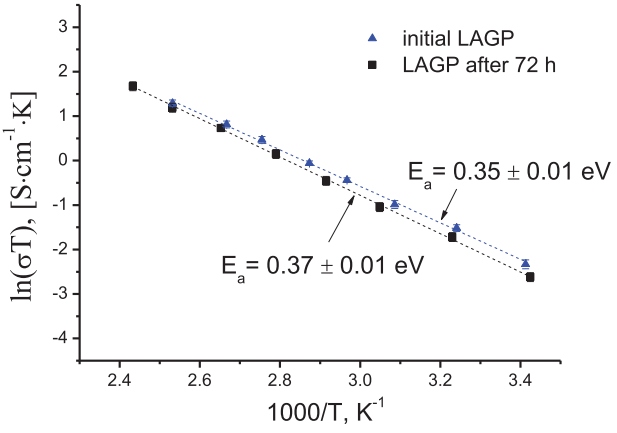

Fig. 7. Temperature dependences of the conductivity of LAGP glass-ceramics before and after holding in metallic Li for 72 h.

ceramics obtained by thermal treatment of monolithic glass has a rather dense microstructure. Fig. 3 demonstrates that the microstructure of all the obtained samples is well-formed and consists of densely packed crystallites of different sizes.

The X-ray powder diffraction patterns of LAGP before and after a contact with molten Li, with and without electrical current applied are given in Fig. 4. The diffraction patterns of the LAGP glass-ceramics electrolyte before and after holding it in metallic Li for 72 h are identical; there are no peaks of the interaction products (Fig. 4). Nevertheless, there are traces of the impurity phase $Li_4P_2O_7$ on the surface of the solid electrolyte after electrochemical cells Li|LAGP|Li have been operating for 9 days. It should be noted that the color of the surface of the glass-ceramic samples and of their fracture surface did not change after a contact with Li in either case. SEM images of cross-sectional profiles of the LAGP glass-ceramics after electrochemical experiments

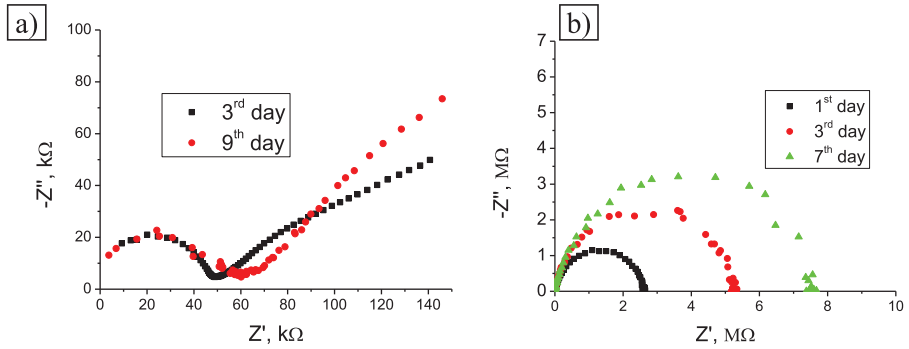

Fig. 8. Impedance plots of *a)* Li|glass-ceramics LAGP|Li and *b)* Li|glass LAGP|Li symmetric cells with the same area of Li electrodes at 200 °C.

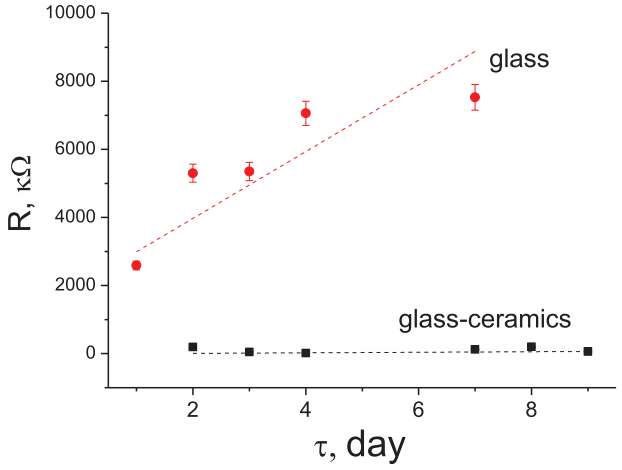

Fig. 9. Electric resistance of Li|glass-ceramic LAGP|Li and Li|glass LAGP|Li cells measured at 200 °C, with the same area of electrodes.

are shown in Fig. 5a and b. The maps of the element distribution of aluminum, germanium, phosphorus, and oxygen (EDAX) on the cross-section sample confirms the absence of new phase formation in glass-ceramics volume in contrast with glass samples, Fig. 5c and d. It can be seen that the morphology and shape of ceramic particles in the surface area and in the volume of glass-ceramics did not change, Figs. 3 and 5. So based on SEM results, stability of the LAGP glass-ceramics versus metallic Li can be confirmed.

Also there are no changes in the NASICON molecular structure as shown in Fig. 6. The shape of the Raman spectra for the obtained LAGP glass-ceramics (Fig. 6) is in good agreement with the literature data for NASICON-type compounds with the space group R-3c studied in the works [15–17]. The Raman spectra of the samples before and after contact with molten Li are identical, which confirms the stability of the obtained NASICON-type glass-ceramics.

Fig. 7 shows Arrhenius plots of temperature dependences of conductivity for LAGP glass-ceramics before and after holding it in Li melt. It can be seen that the conductivity of the electrolyte slightly decreases after a contact with Li, at the same time, the activation energy (E_a) is within the error of measurement, Fig. 7. Thus, holding the investigated electrolyte in molten Li did not lead to its degradation and agrees with the results of XRD, SEM analysis and Raman spectroscopy. According to recorded data, the investigated NASICON-structured LAGP glass-ceramics electrolytes are chemically compatible with metallic Li.

3.3. Impedance spectroscopy investigations

The Cole–Cole plots of Li|glass LAGP|Li and Li|glass-ceramics LAGP|Li cells at 200 °C are given in Fig. 8. The Cole–Cole plots have the typical shapes for monoconducting symmetric cells characterized by the kOhmic resistance values (Fig. 8a), while cells with glass show the resistance values > 2 MΩ (Fig. 8b). During the electrochemical experiment the resistance of Li|glass LAGP|Li cells increases because of the glass interaction with molten Li (see Section 3.1). The plot of Li|glass-ceramics LAGP|Li cell has one semicircle starting from zero point and denoting the resistance value with subsequent Warburg part. Fig. 9 shows that the resistance values of the investigated cell with glass-ceramics do not change significantly over time and do not exceed 200 kΩ, while the resistance of the glass increases sharply from 2.5 to 7.5 MΩ after 7 days of testing. In the case of glass-ceramics the cycling of the symmetrical cell does not lead to the formation of low-conductivity phases, and the appearance of trace amounts of $Li_4P_2O_7$ (Fig. 4) does not have an adverse effect on the functional characteristics of the investigated glass-ceramics. Besides, the color of the glass-ceramics did not change after the experiment. No leakage of molten lithium through glass-ceramic electrolyte was found in vertical measuring cell. A fluctuation of the resistance of the cell with the glass-ceramics was observed during 9 days, which may be the result of poor interface contact. To increase the contact area between the glass-ceramic LAGP electrolyte and lithium anode, a Solid Electrolyte Interphase (SEI) layer should be sputtered, according to [18].

4. Conclusion

Glass of Li_2O–Al_2O_3–GeO_2–P_2O_5 system is not stable in contact with molten metallic lithium. The reaction between glass and lithium gives the product that splits up glass samples. The product might be further fully dissolved in larger amounts of Li melt. A high-conductivity electrolyte $Li_{1.5}Al_{0.5}Ge_{1.5}(PO_4)_3$ with a dense microstructure was obtained by glass crystallization from the glass mentioned above. Glass-ceramics samples possess good stability versus molten lithium in contrast with initial glass. It was shown that the phase composition and molecular structure of the glass-ceramics does not change after a contact with molten lithium. It was established that the resistance values of Li/glass-ceramics LAGP/Li cell though are high enough does not change significantly in time. Glass-ceramics of LAGP can be used as a solid electrolyte in low- and medium-temperature Li power sources with appropriate enhancement of interface behavior and resistance lowering.

Declaration of Competing Interest

The authors declare that they have no known competing financial interests or personal relationships that could have appeared to influence the work reported in this paper.

Acknowledgement

The reported study was funded by the Russian Science Foundation according to the research project No. 18-73-00099. The authors are grateful to Antonov B.D. and Vovkotrub E.G. The research has been carried out with the equipment of the Shared Access Center

“Composition of Compounds” of Institute of High Temperature Electrochemistry of the Ural Branch of the RAS, Ekaterinburg, Russian Federation.

References

[1] Z. Zhang, Y. Shao, B. Lotsch, Y.-S. Hu, H. Li, J. Janek, L.F. Nazar, C.-W. Nan, J. Maier, M. Armand, L. Chen, Energy Environ. Sci. 11 (2018) 1945–1976 https://doi.org/10.1039/C8EE01053F.

[2] P. Knauth, Solid State Ion. 180 (2009) 911–916 https://doi.org/10.1016/j.ssi.2009.03.022.

[3] C. Sun, J. Liu, Y. Gong, D.P. Wilkinson, J. Zhang, Nano Energy 33 (2017) 363–386 https://doi.org/10.1016/j.nanoen.2017.01.028.

[4] F. Zheng, M. Kotobuki, S. Song, M.O. Lai, L. Lu, J. Power Sources 389 (2018) 198–213 https://doi.org/10.1016/j.jpowsour.2018.04.022.

[5] C.J. Leo, B.V.R. Chowdari, G.V. Subba Rao, J.L. Souquet, Mater. Res. Bull. 37 (2002) 1419–1430 https://doi.org/10.1016/S0025-5408(02)00793-6.

[6] X. Xu, Z. Wen, X. Wu, X. Yang, Z. Gu, J. Am. Ceram. Soc. 90 (2007) 2802–2806 https://doi.org/10.1111/j.1551-2916.2007.01827.x.

[7] Y. Meesala, A. Jena, H. Chang, R.-S. Liu, ACS Energy Lett. 2 (2017) 2734–2751 https://doi.org/10.1021/acsenergylett.7b00849.

[8] B. Wu, S. Wang, J. Lochala, D. Desrochers, B. Liu, W. Zhang, J. Yang, J. Xiao, Energy Environ. Sci. 11 (2018) 1803–1810 https://doi.org/10.1039/C8EE00540K.

[9] S. Ramakumar, C. Deviannapoorani, L. Dhivya, L.S. Shankar, R. Murugan, Prog. Mater. Sci. 88 (2017) 325–411 https://doi.org/10.1016/j.pmatsci.2017.04.007.

[10] P. Hartmann, T. Leichtweiss, M.R. Busche, M. Schneider, M. Reich, J. Sann, P. Adelhelm, J. Janek, J. Phys. Chem. C 117 (2013) 21064–21074 https://doi.org/10.1021/jp4051275.

[11] K. He, Y. Wang, C. Zu, Y. Liu, H. Zhao, J. Chen, B. Han, J. Mater. Charact. 80 (2013) 86–91 https://doi.org/10.1016/j.matchar.2013.03.012.

[12] J.K. Feng, L. Lu, M.O. Lai, J. Alloy. Compd. 501 (2010) 255–258 https://doi.org/10.1016/j.jallcom.2010.04.084.

[13] A.M. Cruz, E.B. Ferreira, A.C.M. Rodrigues, J. Non-Cryst. Solids 355 (2009) 2295–2301 https://doi.org/10.1016/j.jnoncrysol.2009.07.012.

[14] D. Safanama, N. Sharma, R.P. Rao, H.E.A. Brand, S. Adams, J. Mater. Chem. A 4 (2016) 7718–7726 https://doi.org/10.1039/C6TA00402D.

[15] B.E. Francisco, C.R. Stoldt, J.-C. M'Peko, Chem. Mater. 26 (2014) 4741–4749 https://doi.org/10.1021/cm5013872.

[16] P. Tarte, A. Rulmont, C. Merckaert-Ansay, Spectrochim. Acta Part A 42 (1986) 1009–1016 https://doi.org/10.1016/0584-8539(86)80012-5.

[17] S.V. Pershina, A.A. Pankratov, E.G. Vovkotrub, B.D. Antonov, Ionics 25 (10) (2019) 4713–4725, https://doi.org/10.1007/s11581-019-03021-5.

[18] X. Yu, A. Manthiram, Energy Environ. Sci. 11 (2018) 527–543 https://doi.org/10.1039/C7EE02555F.